Research Square

Preprints are preliminary reports that have not undergone peer review.
They should not be considered conclusive, used to inform clinical practice,
or referenced by the media as validated information.

Sorption of Ce(III) on magnetic / olive pomace nanocomposite: Isotherm, kinetic and thermodynamic studies

Yusuf Azmi Akbas
Ege University: Ege Universitesi
Sabriye Yusan (sabriyeyusan@gmail.com)
Ege University: Ege Universitesi
Senol Sert
Ege University: Ege Universitesi
Sule Aytas
Ege Universitesi

Research Article

Keywords: olive pomace, magnetite, nanocomposite, cerium, sorption.

Posted Date: March 9th, 2021

DOI: https://doi.org/10.21203/rs.3.rs-179940/v1

License: This work is licensed under a Creative Commons Attribution 4.0 International License.
Read Full License

Sorption of Ce(III) on magnetic / olive pomace nanocomposite: Isotherm, kinetic and thermodynamic studies

Yusuf Azmi Akbas, Sabriye Yusan*, Senol Sert, Sule Aytas

Ege University Institute of Nuclear Sciences 35100 Bornova-Izmir/TURKEY

Corresponding Author: Email: sabriyeyusan@gmail.com, Tel/Fax:+902323113464/+902323886466

Abstract

Used for various high-tech applications, cerium is an important rare earth element (REE) and its sorption on various solids also important considering purification, environmental and radioactive waste disposal, In view of the industrial and environmental terms, it is important to remove Ce^{3+} ions from an aqueous solution. Magnetite and magnetic olive pomace nanocomposite were thus fabricated by a partial reduction co-precipitation approach. The structure and morphological properties of the prepared nano-material and nanocomposite were characterized by means of scanning electron microscopy (SEM), transmission electron microscopy (TEM), X-Ray diffraction (XRD), Fourier transform infrared spectrometry (FT-IR), Vibrating Sample Magnetometry (VSM) and BET surface area analysis. The effects of parameters such as solution pH, contact time, initial Ce(III) concentration and temperature on the sorption efficiency were studied. The maximum sorption capacities of the magnetite (MNP) and magnetic olive pomace nanocomposite (MOP) for Ce(III) ions were found to be 76.92 and 90.90 mgg^{-1}, respectively. The sorption data fitted well with Dubinin- Radushkevich isotherm model and the pseudo-second order kinetic model. Thermodynamic parameters indicated that the sorption was non-spontaneous and endothermic. The present study introduced MNP and MOP as efficient, sustainable adsorbents alternative to commercial ones in wastewater treatment.

Keywords: olive pomace, magnetite, nanocomposite, cerium, sorption.

Introduction

Cerium is the first discovered and the most abundant element of the group of rare earth elements. As well as in combination with other rare earth elements, it is found in the spent nuclear fuel (Dubey and Rao 2011). Cerium accumulates in soil and sediments and its concentration in humans, animals and soils is on the increase. It affects

cell membranes in aquatic animals and has an adverse effect on reproduction and nervous systems. Cerium can also be dangerous for humans. Likely to be encountered in domestic products such as television screens and fluorescent lamps, it causes pulmonary embolism in case of prolonged exposure. The accumulation in human body also endangers the liver (Dubey and Rao 2011).

The waste of the olive oil production process is called the olive pomace, which is obtained in abundance in the Mediterranean countries in particular thanks to large scale production of olive oil. Its high amount makes it important to reuse itself. Olive pomace, is made up of almost all the structural lignocelluloses, as economic and environment friendly biosorbent. Its organic structure contains 37.06% cellulose, 29.39% hemicellulose, 33.65% lignin, which is not harmful to the environment, with a high surface area. Therefore, olive pomace has been the subject of the many studies (Doyurum and Celik 2006).

The most commonly known compound of the iron oxide is Fe_3O_4, which is the most magnetic mineral in the world. Accordingly, it is termed magnetite. Fe_3O_4 nanoparticles caused by precipitation of iron salts in the alkaline environment. Nano magnetite mineral has uses of environment, biomedicine, electromagnetics and science. In its environmental applications, magnetite nanoparticles are used to facilitate separation of sorbent from drinking water and wastewater due to their effective and easily separation features. However, it is known that the coaggregation problem of nanoparticles is often difficult to overcome because the coaggregation reduces the effective surface area of the nanoparticles resulting in reduced reaction activity. In order to solve the problem, magnetic nanoparticles were prepared as a nanocomposite supported by olive pomace (Abdolmohammad et al. 2019). Development of magnetized magnetic biosorbents is of importance for more efficient and easier separation in the sorption process, since the active surface of the magnetite particles attached to the polymeric structure and becomes an important adsorbent to remove heavy metals (Khorasani and Shojaosadati 2019). For sorption of cerium (III) from aqueous solutions, most researchers have used different materials, natural, organic and inorganic; Platanus orientalis leaf powder (Ser et al. 2008), montmorillonite (Klika et al. 2016), ferric oxide (Dubey and Rao 2011), tangerine (Citrus reticulate) peel (Torab-Mostaedi, 2013), granulated zeolites (Suboti and Bronic1986) and Brown Marine Alga (Vijayaraghavan et al. 2010). To the best of our knowledge, the study is the first to show that a magnetic nanocomposite of olive pomace and magnetite is used to adsorb cerium ions from aqueous solutions.

In economic terms, it is very important to dispose of this material obtained as waste from the olive oil production. For such reasons, removal of toxic cerium ions from aqueous solutions is very vital for human and environment health. Therefore, nanocomposite was prepared using magnetic nanoparticles and olive pomace which are

inexpensive and less toxic. Synthesis was conducted by partial reduction co-precipitation which is a simple, effective and economical and environment friendly technique. Adsorbents were then characterized by Scanning Electron Microscopy (SEM), Transmission electron microscopy (TEM), Fourier Transform Infrared Spectroscopy (FT-IR), Vibrating Sample Magnetometry (VSM) and surface area measurements (BET). The effects of various operational parameters on the sorption efficiency for the Ce(III) ions were also studied. Finally, the sorption isotherm models, kinetics and thermodynamics were studied as parameters influencing the sorption capacity and sorption process.

Materials and Methods

Reagents and Materials

The chemicals used are iron (III) chloride ($FeCl_3$, Fluka), sodium sulfite (Na_2SO_3, Merck), hydrochloric acid (HCl, Merck), ammonia (NH_3, Merck) and ethanol (C_2H_5OH, Merck). 3.09 ±0.01 gram of $Ce(NO_3)_3 \cdot 6H_2O$ (Merck) was dissolved separately in one liter of distilled water to prepare the stock solution of cerium with a concentration of 1000 mgL^{-1}. Other concentrations ranging from 25 to 300 mgL^{-1} were prepared by diluting the initial stock solutions with double distilled water. The pH was adjusted by diluted solutions of HNO_3 and NH_4OH. All the chemical reactants were used as Analytical Grade (AR).

The olive pomace extracted using hexane was obtained from the Ege Tarımsal Enerji San. ve Tic. A.Ş., Torbalı, Izmir, TURKEY. Then olive pomace washed by distilled water, dried at room temperature and grounded using a grinding mill to obtain 25 mm in particle size. Then 10 gram of raw olive pomace (OP) was added to 100 mL of 1 M H_3PO_4 solution which was stirred by mechanical stirrer for 24 hours. After the mixing was completed, the solution was washed with distilled water to eliminate the chemical agent excess until the pH reached to neutral and the samples dried in an oven at 60 °C and after stored for later use.

Instrument

Determination of Ce(III) in aqueous solutions was conducted using inductively coupled plasma optical emission spectrometry (ICP-OES) (Perkin Elmer Optima DV 2000). The pH values of all solutions were measured by a Hanna Instrument, model 8521, pH meter. The SEM images were obtained at 5.0 kV on a field emission scanning electron microscope (Philips XL 30S FEG). Studies of the transmission electron microscopy (TEM) were performed using Jem Jeol 2100F 200kV HRTEM under the 200kV and FEI Tecnai G^2 Spirit Bio (TWIN) CTEM under the 120kV. FT-IR spectra were recorded in the 4400–400 cm^{-1} spectral region by means of a Thermo FT-IR

spectrometer. Magnetic measurements of the samples in the powder form were carried out at room temperature using a vibrating sample magnetometry (VSM) (Lakeshore 7407). N_2-BET adsorption–desorption were determined using Micromeritics ASAP 2020 equipment at 77 K, for specific surface area and porosity evaluation for magnetic nanoparticles and magnetic olive pomace nanocomposite. The adsorption experiments were studied by batch technique using a thermostated shaker water bath, model GFL-1083.

Synthesis of Magnetic nanoparticles and Nanocomposite

The magnetic nanoparticles (MNP) and magnetic olive pomace (MOP) nanocomposite were prepared by partial reduction co-precipitation, as reported in the literature (Yusan et al. 2014).

The olive pomace sample was chemically modified with phosphoric acid (H_3PO_4) as follows: 10 g- raw olive pomace was added to 100 mL of 1 M H_3PO_4 which the solution was stirred with mechanical stirrer for 24 hours. After the mixing was completed, the solution was washed with distilled water to eliminate the chemical agent excess until the pH reached neutral and the samples were dried in an oven at 60 °C and after stored for later use. 1 g modified (with phosphoric acid) olive pomace was used in the synthesis of the nanocomposite.

Firstly, N_2 gas was bubbled through distilled water used in synthesis to remove dissolved oxygen for 5 min. To prepare the magnetic olive pomace nanocomposite, $FeCl_3$ was dissolved in 2.0 M HCl and transferred to a 500 mL three-neck flask and diluted with 100 mL distilled water. Later, freshly prepared 0.08 M Na_2SO_3 was added slowly under nitrogen atmosphere. Afterwards, 1.0 g modified olive pomace was poured into the three-neck flask with a mixture of 3.0 M 6.0 mL of iron chloride solution in it. 8 mL of NH_3 solution (28%, w/v) was gently added to the mixture under nitrogen atmosphere then diluted with distilled water (25 mL). The solution was later allowed to stand at 70 °C for 15–30 min and black precipitate was collected with a magnet and washed by distilled water until the pH of the suspension reached to 7.0, and then continued to wash with water–ethanol (2/1, v/v) mixture. The precipitate was dried at vacuum in 45 °C and used for the characterization.

Sorption Experiments

Sorption was carried out in thermostatic water bath shaker using 10 mL of Ce(III) solutions at the appropriate concentrations and 0.04 g of adsorbent by batch technique. The effects of sorption parameters such as contact time (5–240 min), pH (1–6), Ce(III) concentration (25–300 mgL^{-1}) and temperature (30–50 °C) on the sorption of Ce(III) were determined by changing a parameter and keeping others constant. After sorption, the solution was vacuum filtered through the membrane filters and the Ce(III) concentrations in the solutions were determined using

the ICP-OES instrument. Solutions of 10, 25, 50, 100 mgL^{-1} Ce(III) concentration and 150, 250, 300 mgL^{-1} for higher concentrations were used as standard for calibration in ICP-OES instrument.

The isothermal studies were performed by changing the initial cerium concentration from 25 to 300 mgL^{-1}, while the rest of the parameters were kept at their optimal values.

The sorption kinetics were realized at 50 mgL^{-1} cerium concentration from 5 to 240 min contact time at 25 °C. The sorption capacity of Ce(III) ions sorbed per gram sorbent (qe, mgg^{-1}) and sorption efficiency (Sorp.%), according to the obtained data are calculated in the followings:

$$Sorption(\%) = \frac{(C_0 - C_e)}{C_e} \times 100 \qquad (1)$$

$$q_e = \frac{(C_i - C_e)V}{W} \qquad (2)$$

C_0: initial concentration of adsorbate (mgL^{-1}); C_e: equilibrium concentration of adsorbate (mgL^{-1}) W the mass of the adsorbent (g) and V the volume of the aqueous phase (mL). All the experiments were performed in duplicates with experimental errors within ±3%.

Results and Discussion

Characterization

The morphology of magnetic olive pomace was analyzed by SEM in Figure 1. Surface image of MOP showed agglomeration of spherical shaped Fe_3O_4 nanoparticles with varying sizes. It can be concluded that Fe_3O_4 nanoparticles are attached to the surface of the olive pomace.

Fig. 1. SEM images of magnetite-olive pomace nanocomposite (MOP) with various magnifications

Figure 2(A) and (B) illustrates the TEM images of magnetite and magnetite-olive pomace nanocomposite, respectively. They show that pure magnetite nanoparticles were being more uniform after supported by olive pomace and also Fig. 2(B) indicates that Fe_3O_4 nanoparticles are well decorated and clearly observed. Due to filling of magnetite particles aggregate with olive pomace, the specific surface area of nanocomposite decreased (Pylypchuk et al. 2016).

Fig. 2. TEM images of MNP (A) and MOP (B)

Brunauer-Emmett-Teller (BET) analysis was performed to investigate the specific surface area of the magnetic nanocomposite. The BET surface area of the nanocomposite was found to be 120.37 $m^2 g^{-1}$. The literature found surface area of pure magnetite between 134 and 286.9 $m^2 g^{-1}$ (Pylypchuk et al. 2016; Ardelean et al. 2017; Ma et al., 2014). Moreover, the surface area of the raw olive pomace was measured as 0.90 $m^2 g^{-1}$, according to which the surface area of the nanocomposite formed by magnetite with olive pomace can be concluded to be significantly increased.

The FT-IR spectra of MOP and Ce:MOP are described in Figure 3.In addition, the previous study showed that olive pomace and modified olive pomace spectra were provided to see the difference of the adsorbents (Akbas and Yusan 2020). In the FTIR spectrum of magnetite olive pomace, the band at 1646 cm^{-1} was attributed to stretching vibrations of the O-H functional groups in the structure of the adsorbents (Ahmadi et al. 2020). In addition, the bands were at 1428 cm^{-1} and 1406 cm^{-1} for C–H bending vibrations for MOP and Ce:MOP, respectively. Magnetite adsorption bands can be observed at 581 cm^{-1} (Pylypchuk et al. 2016). The band at 558 cm^{-1} was associated to the Fe-O vibration characteristic of the magnetite phase, which was the main band for both spectra. From the Fig. 3, it follows that all the peaks shifted slightly after the biosorption of the Ce(III) ions, for example Fe-O band shifted from 558 cm^{-1} to 552 cm^{-1} (Iconaru et al. 2016). The shifting of absorption bands towards low wavelength shows the presence of physical forces between nanocomposite and Ce(III) ions (Muhammad et al. 2019).

Fig. 3. FTIR spectra of MOP and Ce:MOP after the biosorption of Ce ions

The magnetic properties of the magnetite nanoparticles and magnetic olive pomace nanocomposite were determined at room temperature. According to VSM results from Fig.4, saturation magnetization was found 20.13 and 16.15 $emug^{-1}$ for the magnetite and magnetic nanocomposite, respectively. It can be concluded that both sorbents are super-paramagnetic. The magnetization value for magnetite-olive pomace nanocomposite was less than magnetite nanoparticles due to the presence of olive pomace onto the body of nanoparticles. Although magnetization of nanocomposite in the saturation was lower than magnetite, magnetic separation of MOP was still rapid.

Fig. 4. Hysteresis loops of the MNP and MOP

The XRD analysis was also used to determine the crystalline structure of the material, whose results for the MNP and MOP composite are shown in Fig. 5. In the MNP, the peaks at 2θ values of 30.2; 35.4; 43.3; 53.5; 57.2 and 63.0 are quite identical to characteristic peaks of the Fe_3O_4 crystal with the cubic spinal structure for magnetic olive pomace composite which is in good agreement with the value in the literature (JCPDS card No. 19-0629) (Yusan et al. 2014; Boushehrian et al. 2020; Azari et al. 2017) which are marked by 220, 311, 400, 422, 511, and 440 indices, respectively. After the formation of magnetic olive pomace composite, the intensities of the peaks for composite were decreased and composite structure was not in a good crystalline form due to the olive pomace incorporation.

Fig. 5. XRD pattern of the MNP and MOP

Sorption Experiments

Effect of pH

The solution pH plays a major role in the removal of adsorbents from aqueous solutions since its effect on the surface charge of the adsorbent, the degree of ionization and the speciation of adsorbate and surface functional groups influence the sorption process. The impact of pH on the sorption capacity of synthesized materials was studied using solution of 100 mgL^{-1} Ce(III) at a pH range of 1.0–6.0 (at pH >6.5, Ce(III) ions precipitated) at 25 °C for 120 min (Iconaru et al. 2016; Kutahyalı et al. 2012). The results of the experiment are in Fig. 6. As seen from Figure 6, maximum Ce(III) uptake was obtained at pH 6.0 for magnetite (MNP) and magnetite-olive pomace nanocomposite (MOP) as 12.22 mgg^{-1} and 13.93 mgg^{-1}, respectively. The results from Figure 6 suggested that the sorption capacity of MOP was better than MNP could be associated with the lignocellulosic structure of the olive pomace.

Fig. 6. Influence of pH on sorption of Ce(III) ions by the MNP and MOP nanocomposite (m: 0.04 g, c: 100 mgL^{-1}, v: 10 mL, t: 2 h)

Effect of Contact Time

Contact time is an important parameter for investigation of the sorption process. The sorption experiments were carried out for contact times ranging from 5 to 240 min with fixed amounts of adsorbent (0.04 g) at ambient temperature (25 °C) with all other parameters were kept constant (Figure 7).

Fig. 7. Influence of contact time on sorption of Ce(III) ions by the MNP and MOP nanocomposite (m: 0.04 g, c: 100 mgL^{-1}, v: 10mL, pH:6.0)

As seen from Figure 7, sorption was initially fast and occupied selectively the active sites on the adsorbents. The active sites on the adsorbents were filled when the contact time was increased and the sorption of Ce(III) onto adsorbents reached to an equilibrium (Gunasundari et al. 2017; Pearlin et al. 2014). For further experiments, the optimum contact time was selected 30 and 45 minutes for MNP and MOP, respectively.

Effect of Initial Ce(III) Concentration

The influence of the Ce(III) concentration on adsorption was investigated in a range from 25 to 300 mgL^{-1}. The results are exhibited in Figure 8. The sorption capacities of cerium(III) by MNP and MOP were found 6.20 mgg^{-1} and 12.57 mgg^{-1} , respectively. The higher sorption capacity of the MOP might be contributed to by cellulose, hemicellulose and lignin contents of the magnetic nanocomposite. For both sorbents, sorption capacity increases with the Ce(III) initial concentration and then they reach an equilibrium, which can be explained by the theory that the mass transfer driving force at the solid-liquid interface is enhanced as the initial concentration increases.

Fig. 8. Influence of initial concentration of Ce(III)ions by the MNP and MOP nanocomposite

Thermodynamic studies

Fig. 9 shows the effect of temperature and thermodynamic features on the sorption of cerium on the MNP and MOP nanocomposite. Thermodynamic parameters such as changes of enthalpy (ΔH°), entropy (ΔS°) and free energy (ΔG°) were estimated by the following and given in Table 1.

$$lnK_d = \frac{\Delta S^o}{R} - \frac{\Delta H^o}{RT} \quad (3)$$

$$\Delta G^o = \Delta H^o - T\Delta S^o \quad (4)$$

$$K_d = \frac{q_e}{C_e} \quad (5)$$

Fig. 9. lnK_d versus temperature graph of Ce(III) sorption by the MNP (a) and MOP (b) nanocomposite

Table 1. Thermodynamics parameters of Ce(III) sorption

Analysis of thermodynamic parameters not only judges the nature of adsorption process but also provides the information on predominant mechanisms in the adsorption reaction (e.g., physical interaction, chemical interaction) (Yan et al. 2020). The positive value of the enthalpy change suggests the endothermic nature of the sorption process for MNP and MOP. The positive value of ΔS^0 due to the exchange of the Ce(III) ions with more mobile ions present on the exchanger, which would lead to increase in the entropy in the sorption process (Tamjidi et al. 2019). The positive values of ΔG^0 suggested that Ce (III) sorption at various temperatures was

thermodynamically non-spontaneous in nature for the both sorbents (Ahmad et al. 2011; Haroon et al. 2016; Yi et al., 2017; Sangkarak et al. 2020). ΔH° and ΔS° values were positive, confirming that adsorption system of Ce(III) onto the MNP and MOP at the test temperatures was endothermic. It was expected that the degree of randomness at the solid–liquid interface would increase during the adsorption system. Moreover, similar evidence was found for the heavy metal adsorption (Haroon et al. 2016; Sangkarak et al. 2020; Schneider et al. 2007). When the value of ΔH° is lower than 40 $kJmol^{-1}$, the type of sorption can be accepted as a physical process. The values of ΔH° were calculated as 5.7872 $kJmol^{-1}$ and 7.4495 $kJmol^{-1}$ for MNP and MOP, respectively. They indicate that the sorption was physical by nature and thus involved weak forces of attraction (Ho and McKay 1999), which is consistent with the results of the isotherm models. Furthermore, uptake of cerium can be concluded to be slightly increases at temperature increasing (Kaveeshwar et al. 2018).

Adsorption Isotherms

The Langmuir, Freundlich and Dubinin-Radushkevich (D-R) isotherm models were applied to obtain data of Ce(III) sorption mechanism on MNP and MOP nanocomposite surface. The isotherm equations and the results are presented in Tables 2 and 3, respectively. The calculated maximum capacity (mgg^{-1}) express the total capacity of the sorbent for cerium and the R_L values were calculated within the range of 0–1 confirming the favorable character of the uptake of the cerium by the adsorbents (Anitha et al. 2015). Table 3 shows that D-R isotherm model (0.9981) was very suitable for describing the sorption equilibrium of cerium by the magnetic olive pomace nanocomposite. Otherwise, Freundlich isotherm model (0.9944) and D-R isotherm model (0.998) are fitted very well for MNP. Therefore, it can be inferred that the sorption process followed both isotherm models. According to the affinity of the interaction between adsorbent and adsorbate can be explained by the value of the sorption intensity (n) by the Freundlich isotherm model, the value $1 < n < 10$ illustrates that sorption tends to be favored. The importance of n is given as follows: $n < 1$ (chemical process); $n = 1$ (linear); $n > 1$ (physical process) (Saravan et al. 2018). As seen from the Table 3, n values are in the same range for both of the sorbent and n value is higher than 1. Accordingly, it can be concluded that physical sorption is favorable for both adsorbents.

Table 2. Utilized isotherms models (linear) in sorption studies

q_{eq}, C_{eq} equilibrium concentrations of cerium in solid and liquid phase, respectively; Q_o is the maximum sorption capacity (mgg^{-1}); b_L is the Langmuir constants are related to sorption energy. K_F is the sorption capacity of sorbent

(mgg^{-1}) and n_F a constant related to sorption intensity (dimensionless) for Freundlich isotherm model. C_{ads} (molg^{-1}) is the amount of solute sorbed per unit weights of solid, X_m (molg^{-1} or mgg^{-1}) the sorption capacity, β (molJ^{-1})^2 a constant related to energy and $\mathcal{E}$ the Dubinin–Radushkevich isotherm constant. This approach is generally used to distinguish whether the physical and chemical adsorption of metal ions is by the mean free energy, E per molecule of adsorbate, which can be calculated by the relationship Dada et al. 2012).

Using the linear plot of D-R isotherm model, X_m was determined to 0.0050 and 0.0053 molg^{-1}, the mean free energy, E= 7 kJmol^{-1} and 6.93 kJmol^{-1} for MNP and MOP, respectively. These results indicates physiosorption process for both sorbents (Sentil Kumar et al. 2011).

Table 3. Constants of isotherm and correlation of Ce(III)

Unfortunately, there is no related information about Ce(III) sorption on magnetite olive pomace nanocomposite. Sorption capacities of the MNP and MOP nanocomposite can be compared with those of sorbents in the literature for Ce(III) sorption (Table 4). The results below indicate the maximum sorption capacities from the study can be comparable with those in the literature ranging from 12.08 mgg^{-1} to 180.2 mgg^{-1} for Ce(III).

Table 4. Comparative of Ce(III) capacities with the literature

Adsorption kinetics

The present study used two kinetic models to investigate the mechanism of sorption and rate-controlling processes, such as mass transfer and/or chemical reaction. The linear forms of the pseudo-first-order and pseudo-second-order equations are in the following equations, respectively:

$$\log(q_e - q_t) = log q_e - \frac{k_1 t}{2{\cdot}303} \qquad (6)$$

$$\frac{t}{q_t} = \frac{1}{k_2 q_e^2} + \frac{t}{q_e} \qquad (7)$$

where q_e and q_t (mgg^{-1}) are the amounts of adsorbate adsorbed at equilibrium and at any time, t (h), k_1 (1/h) and k_2 (g mgh^{-1}) the equilibrium rate constants of pseudo-first-order and pseudo-second-order models and t (h) the contact time, respectively.

In the present work, the kinetic experiments of Ce(III) sorption onto MNP and MOP were analyzed using the pseudo-first-order (not shown) and pseudo-second-order kinetic models with results in Fig. 10.

The linear plot of log (q_e - q_t) versus t provides a slope of k_1 and intercept of log q_e. The values of k_1 and R^2 from the plot for sorption of Ce(III) on the adsorbents are shown in Table 5.

According to two the kinetic models, the calculated constants for the sorption kinetics are in Table 5. The R^2 values for the pseudo-first-order model for both adsorbents were not high, which shows that the sorption of Ce(III) on the adsorbents does not follow a pseudo first order kinetic model. Based on Table 5, R^2 values obtained from the pseudo second-order model were high and q_e values are in good agreement with the experimental results. It is clear that the sorption of Ce(III) on MNP and MOP fits this model well and sorption process is controlled by different sorption mechanisms, such as surface complexation, ion exchange, etc (Alslaibi et al. 2013; Lazarević et al. 2010; Hubbe et al. 2019).

Fig. 10. Plot of pseudo-second order kinetic model for sorption of Ce(III) onto MNP and MOP

Table 5. Kinetic parameters of pseudo-first and pseudo-second order models for the sorption of Ce(III) onto MNP and MOP

Conclusion

The study synthesized magnetic olive pomace nanocomposite by means of partial reduction co-precipitation method. Characterization of the nanocomposite was carried out by analyses of FTIR, SEM, TEM, VSM and BET. The SEM and TEM pictures showed magnetic particles located on the olive pomace surface. The BET surface area of the nanocomposite was found as 120.37 m^2g^{-1}. According to VSM results, MNP and MOP were superparamagnetic and saturation magnetization 20.13 and 16.15 $emug^{-1}$. The sorption of Ce(III) ions was studied on magnetite and magnetic olive pomace using batch technique under different experimental conditions. According to the results, optimum operation conditions were determined as pH of 6.00, at 45-minute contact time, 100 mgL^{-1} Ce(III) concentration and 40 °C and pH of 6.00, at 30 minutes contact time, 50 mgL^{-1} Ce(III) concentration and 40 °C for MOP and MNP, respectively. The maximum sorption capacities of MNP and MOP for Ce(III) were found to be 76.92 mgg^{-1} and 90.90 mgg^{-1} , respectively. They were higher than previous reported adsorbents for Ce(III) removal. Based on the results from in the present research, the value of the parameter E for the sorption process was lower than 8 kJ/mol for the adsorbents, leading to the conclusion that the sorption process was found on a physical basis. According to the results of the equilibrium study, one can infer that the cerium ion adsorption on the studied adsorbents is a favorable physical process where the equilibrium data follows the Freundlich isotherm model. In the meantime, according to results from the kinetic and thermodynamic study, the sorption process is controlled by different sorption mechanisms, such as surface complexation, ion exchange and electrostatic attraction are the contributions to the effective removal of Ce(III) ions. From the study, it was clear

that magnetite/olive pomace nanocomposite could be an effective biosorbent for Ce(III) removal from aqueous media, based on which synthesized adsorbents have good magnetic property related to the magnetic field for easy removal of adsorbent from the aqueous solutions. Therefore, it can be considered that these adsorbents can be used as an effective one to effectively remove Ce ions from wastewater.

Data availability

The datasets used and/or analyzed in this study are available by the corresponding author on reasonable request (sabriyeyusan@gmail.com).

Acknowledgements

We would like to express our deep gratitude to Dr. Berkan Cetinkaya and Dr. Emine Nostar Aslan for BET and FTIR analysis in Ege University Institute of Nuclear Sciences.

Funding

This study was financially supported by by Ege University Scientific Research Project Unit Project No. 2016 NBE 002.

Author information

Affiliations

Ege University Institute of Nuclear Sciences 35100 Bornova-Izmir/TURKEY

Yusuf Azmi Akbas, Sabriye Yusan, Senol Sert & Sule Aytas

Contributions

Yusuf Azmi Akbas: Synthesis of the materials, realization of the experiments, calculations.

Sabriye Yusan: Supervision, data acquisition, methodology and writing - review and editing.

Senol Sert: Measurements of the Ce ions by ICP-OES.

Sule Aytas: Data analysis and writing - review and editing.

Ethics declarations

Conflict of interest

The authors declare that they have no conflict of interest.

Ethical approval

Not applicable: our manuscript does not report on or involve the use of any animal or human data or tissue.

Consent to participate

Not applicable

Consent to publish

Not applicable

References

Abdolmohammad-Zadeh H, Ayazi Z, Naghdi Z (2019) Nickel oxide/chitosan nano-composite as a magnetic adsorbent for preconcentration of Zn(II) ions. J Magn Magn Mater 488:165311.

Ahmad MA, Rahman NK (2011) Equilibrium, kinetics and thermodynamic of Remazol Brilliant Orange 3R dye adsorption on coffee husk-based activated carbon. Chem Eng J 170: 154-161.

Ahmadi A, Foroutan R, Esmaeili H et al (2020) The role of bentonite clay and bentonite clay@MnFe2O4 composite and their physico-chemical properties on the removal of Cr(III) and Cr(VI) from aqueous media. Environ Sci Pollut Res 27:14044-14057.

Akbas YA, Yusan S (2020) Development and characterization of non-treated and chemically modified olive pomace biosorbents to remove Ce(III) ions from aqueous solutions. J Radioanal Nucl Chem 323:763–772.

Alslaibi TM, Abustan I, Ahmad MA et al (2013) Cadmium removal from aqueous solution using microwaved olive stone activated carbon. J Environ Chem Eng 1:589-599.

Anitha T, Senthil Kumar P, Sathish Kumar K (2015) Binding of Zn(II) Ions to Chitosan–PVA Blend in Aqueous Environment: Adsorption Kinetics and Equilibrium Studies. Environ Prog Sustain 34:15-22.

Ardelean IL, Stoencea LBN, Ficai D et al (2017) Development of Stabilized Magnetite Nanoparticles for Medical Applications. J Nanomater Article ID 6514659:9 pages.

Azari A, Gharibi H, Kakavandi B et al (2017) Magnetic adsorption separation process: an alternative method of mercury extracting from aqueous solution using modified chitosan coated Fe3O4 nanocomposites. J Chem Technol Biotechnol 92:188–200.

Behdani FN, Rafsanjani AT, Torab-Mostaedi M et al (2013) Adsorption ability of oxidized multiwalled carbon nanotubes towards aqueous Ce(III) and Sm(III). Korean J Chem Eng 30:448-455.

Boushehrian MM, Esmaeili H, Foroutan R (2020) Ultrasonic assisted synthesis of Kaolin/CuFe2O4 nanocomposite for removing cationic dyes from aqueous media. J Environ Chem Eng 8:103869.

Chen T, Yan C, Wang Y et al (2015) Synthesis of activated carbon-based amino phosphonic acid chelating resin and its adsorption properties for Ce(III) removal. Environ Technol 36:2168-2176.

Dada AO, Olalekan AP, Olatunya AM et al (2012) Langmuir, Freundlich, Temkin and Dubinin–Radushkevich Isotherms Studies of Equilibrium Sorption of Zn2+ Unto Phosphoric Acid Modified Rice Husk. IOSR J Appl Chem 3:38-45.

Dubey SS, Rao BS (2011) Removal of cerium ions from aqueous solution by hydrous ferric oxide – A radiotracer study. J Hazard Mater 186:1028-1032.

Dorabei RZ, Jalalat V, Tadjarodi A (2016) Central composite design optimization of Ce(III) ion removal from aqueous solution using modified SBA-15 mesoporous silica. NJC 40:5128-5134.

Doyurum S, Celik A (2006) Pb(II) and Cd(II) removal from aqueous solutions by olive cake. J Hazard Mater B138:22–28.

Gunasundari E, Senthil Kumar, P (2017) Adsorption isotherm, kinetics and thermodynamic analysis of Cu(II) ions onto the dried algal biomass (Spirulina platensis). J Ind Eng Chem 56:129-144.

Haroon H, Ashfaq T, Gardazi SMH et al (2016) Equilibrium kinetic and thermodynamic studies of Cr(VI) adsorption onto a novel adsorbent of Eucalyptus camaldulensis waste: batch and column reactors. Kor J Chem Eng 33:2898-2907.

Ho YS, McKay G (1999) Pseudo-Second Order Model for Sorption Processes. Process Biochem 34:451-465.

Hubbe MA, Azizian S, Douven S (2019) Implications of apparent pseudo-second-order adsorption kinetics onto cellulosic materials: A review. BioRes 14:7582-7626.

Iconaru SL, Guégan R, Popa C et al (2016) Magnetite (Fe3O4) nanoparticles as adsorbents for As and Cu removal. Appl Clay Sci 134:128-135.

Kaveeshwar Ar, Ponnusamy SK, Revellamec ED et al (2018) Pecan shell based activated carbon for removal of iron(II) from fracking wastewater: Adsorption kinetics, isotherm and thermodynamic studies. Process Saf Environ Prot 14:107–122.

Khorasani AC, Shojaosadati SA (2019) Magnetic pectin-Chlorella vulgaris biosorbent for the adsorption of dyes. J Environ Chem Eng 7(3):103062.

Klika K, Seidlerová J, Valášková M et al (2016) Uptake of Ce(III) and Ce(IV) on montmorillonite. Appl Clay Sci 132–133:41–49.

Kutahyalı C, Sert S, Cetinkaya B et al (2012) Biosorption of Ce(III) onto modified Pinus brutia leaf powder using central composite design. Wood Sci Technol 46:721-736.

Lazarevic´ S, Jankovic´-Cˇastvan I, Djokic´ V et al (2010) Iron- Modified Sepiolite for Ni2+ Sorption from Aqueous Solution: An Equilibrium, Kinetic, and Thermodynamic Study. J Chem Eng Data 55:5681-5689.

Ma J, Wang L, Wu Y et al (2014) Facile Synthesis of Fe3O4 Nanoparticles with a High Specific Surface Area. Mater Trans 55:1900-1902.

Muhammad A, Shah AA, Bilal S et al (2019) Basic Blue Dye Adsorption from Water Using Polyaniline/Magnetite (Fe3O4) Composites: Kinetic and Thermodynamic Aspects. Materials 12:1-26.

Pearlin Kiruba U, Senthil Kumar P, Prabhakaran C et al (2014) Characteristics of thermodynamic, isotherm, kinetic, mechanism and design equations for the analysis of adsorption in Cd(II) ions-surface modified Eucalyptus seeds system. J Taiwan Inst Chem E 45:2957-2968.

Pylypchuk V, Kołodyńska D, Kozioł M et al (2016) Gd-DTPA Adsorption on Chitosan/Magnetite Nanocomposites. Nanoscale Res Lett 11:168-177.

Sadovsky D, Brenner A, Astrachan B et al (2016) Biosorption potential of cerium ions using Spirulina biomass. J Rare Earths 34:644-652.

Sangkarak S, Phetrak A, Kittipongvises S et al (2020) Adsorptive performance of activated carbon reused from household drinking water filter for hexavalent chromium-contaminated water. J Environ Manage 272:111085.

Saravanan A, Senthil Kumar P, Annam Renita A (2018) Hybrid synthesis of novel material through acid modification followed ultrasonication to improve adsorption capacity for zinc removal. J Clean Prod 172:92-105.

Schneider RM, Cavalin CF, Barros MASD et al (2007) Adsorption of chromium ions in activated carbon. Chem Eng J 132:355-362.

Serunting MA, Rusnadi R, Setyorini DA et al (2018) An effective cerium (III) ions removal method using sodium alginate-coated magnetite (Alg-Fe3O4) nanoparticles. J Water Supply Res T 67:754-765.

Shojaei Z, Iravani E, Moosavian MA et al (2016) Removal of Cerium from Aqueous Solutions by Amino Phosphate Modified Nano TiO2: Kinetic, and Equilibrium Studies. Iranian J Chem Eng 13:3-21.

Senthil Kumar P, Ramalingam S, Abhinaya RV et al (2011) Lead(II) Adsorption onto Sulphuric Acid Treated Cashew Nut Shell. Separ Sci Technol 46:2436-2449.

Sert Ş, Kütahyalı C, İnan S et al (2008) Biosorption of lanthanum and cerium from aqueous solutions by Platanus orientalis leaf powder. Hydrometallurgy 90: 13-18.

Suboti B, Bronic J (1986) Removal of cerium(III) species from solutions using granulated zeolites. J Radioanal Nucl Chem 102:465-481.

Tamjidi S, Esmaeili H, Moghadas BK (2019) Application of magnetic adsorbents for removal of heavy metals from wastewater: a review study. Mater Res Express 6:102004.

Torab-Mostaedi M (2013) Biosorption of Lantanum and Cerium from Aqueous Solutions Using Tangerine (Citrus reticulata) Peel: Equilibrium, Kinetic and Thermodynamic Studies. Chem Ind Chem Eng Q 19:79−88.

Torab-Mostaedi M, Asadollahzadeh M, Hemmati A et al (2015) Biosorption of lanthanum and cerium from aqueous solutions by grapefruit peel: equilibrium, kinetic and thermodynamic studies. Res Chem Intermed 41:559-573.

Varsihini CJS, Das D, Das N (2014) Optimization of parameters for cerium(III) biosorption onto biowaste materials of animal and plant origin using 5-level Box-Behnken design: Equilibrium, kinetic, thermodynamic and regeneration studies. J Rare Earth 32:745-758.

Vijayaraghavan K, Sathishkumar M, Balasubramanian R (2010) Biosorption of Lanthanum, Cerium, Europium, and Ytterbium by a Brown Marine Alga, Turbinaria Conoides. Ind Eng Chem Res 49:4405-4411.

Vijayaraghavan K, Balasubramanian R (2010) Single and binary biosorption of cerium and europium onto crab shell particles. Chem Eng J 163:337-343.

Yan Y, Sarkar B, Zhou L et al (2020) Phosphorus-rich biochar produced through bean-worm skin waste pyrolysis enhances the adsorption of aqueous lead. Environ Pollut 266:115177.

Yi Y, Lv J, Liu Y et al (2017) Synthesis and application of modified Litchi peel for removal of hexavalent chromium from aqueous solutions. J Mol Liq 225:28-33.

Yusan S, Korzhynbayeva K, Aytas S et al (2014) Preparation and investigation of structural properties of magnetic diatomite nanocomposites formed with different iron content. J Alloys Comp 608:8-13.

Figures

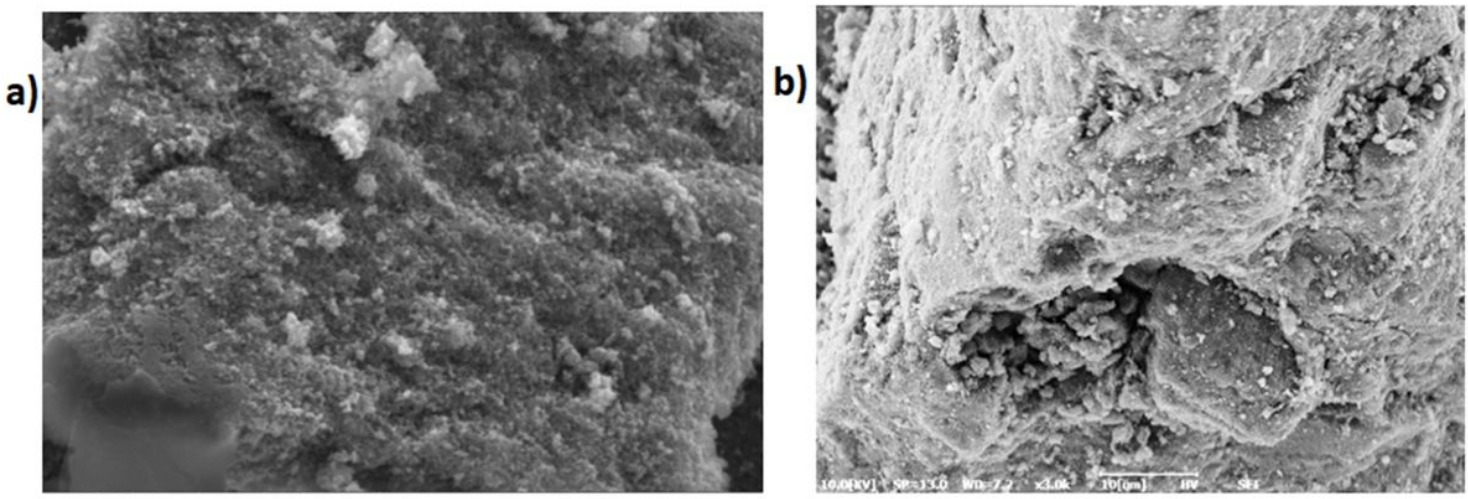

Figure 1

SEM images of magnetite-olive pomace nanocomposite (MOP) with various magnifications

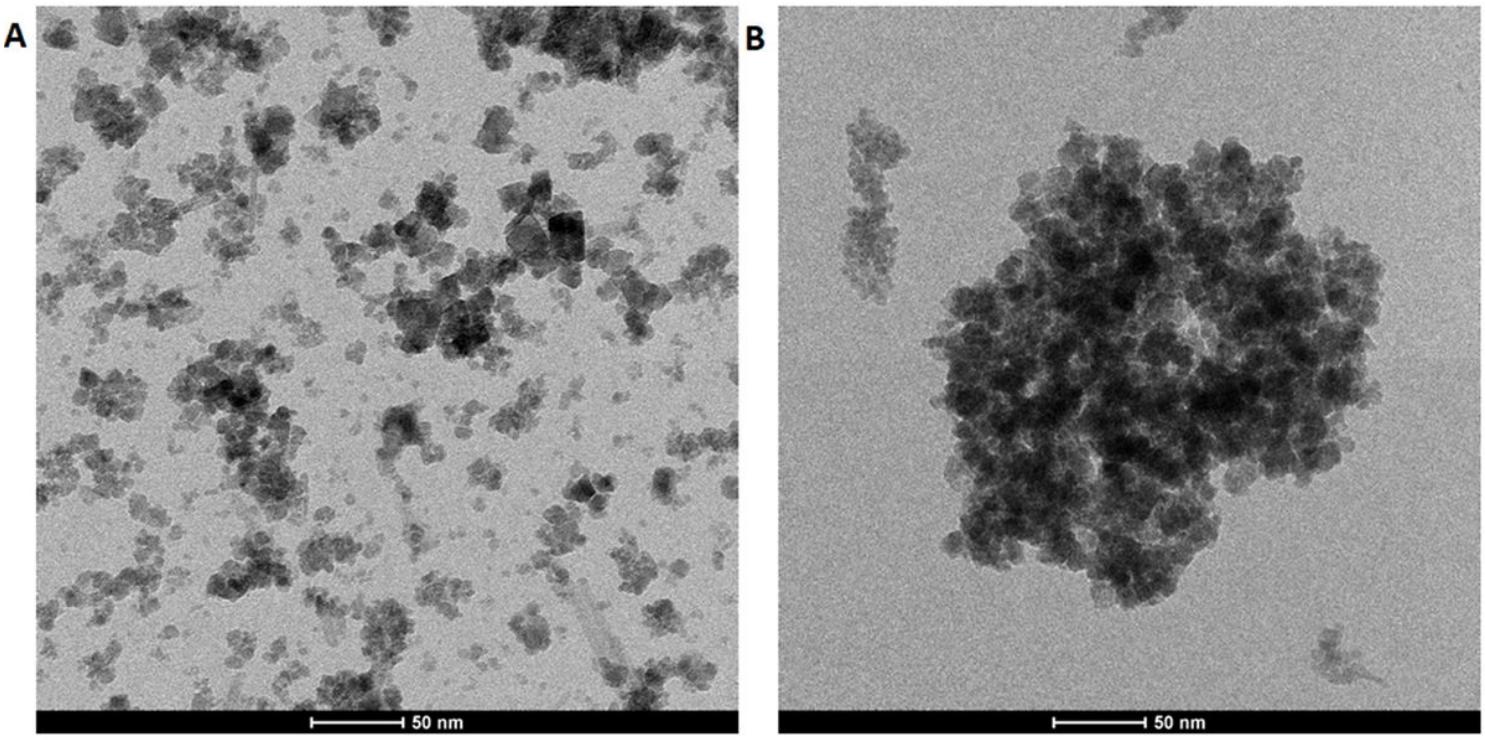

Figure 2

TEM images of MNP (A) and MOP (B)

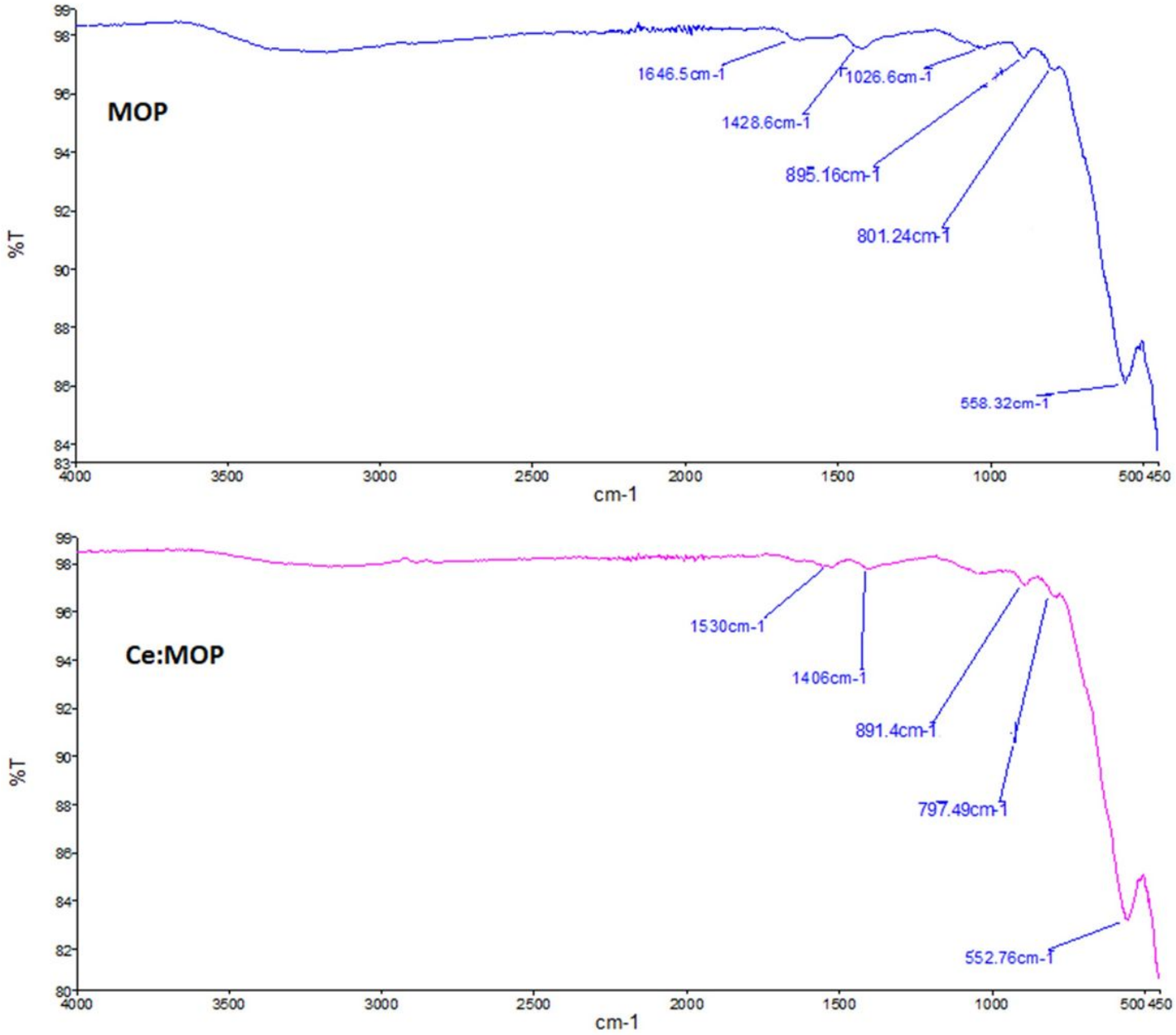

Figure 3

FTIR spectra of MOP and Ce:MOP after the biosorption of Ce ions

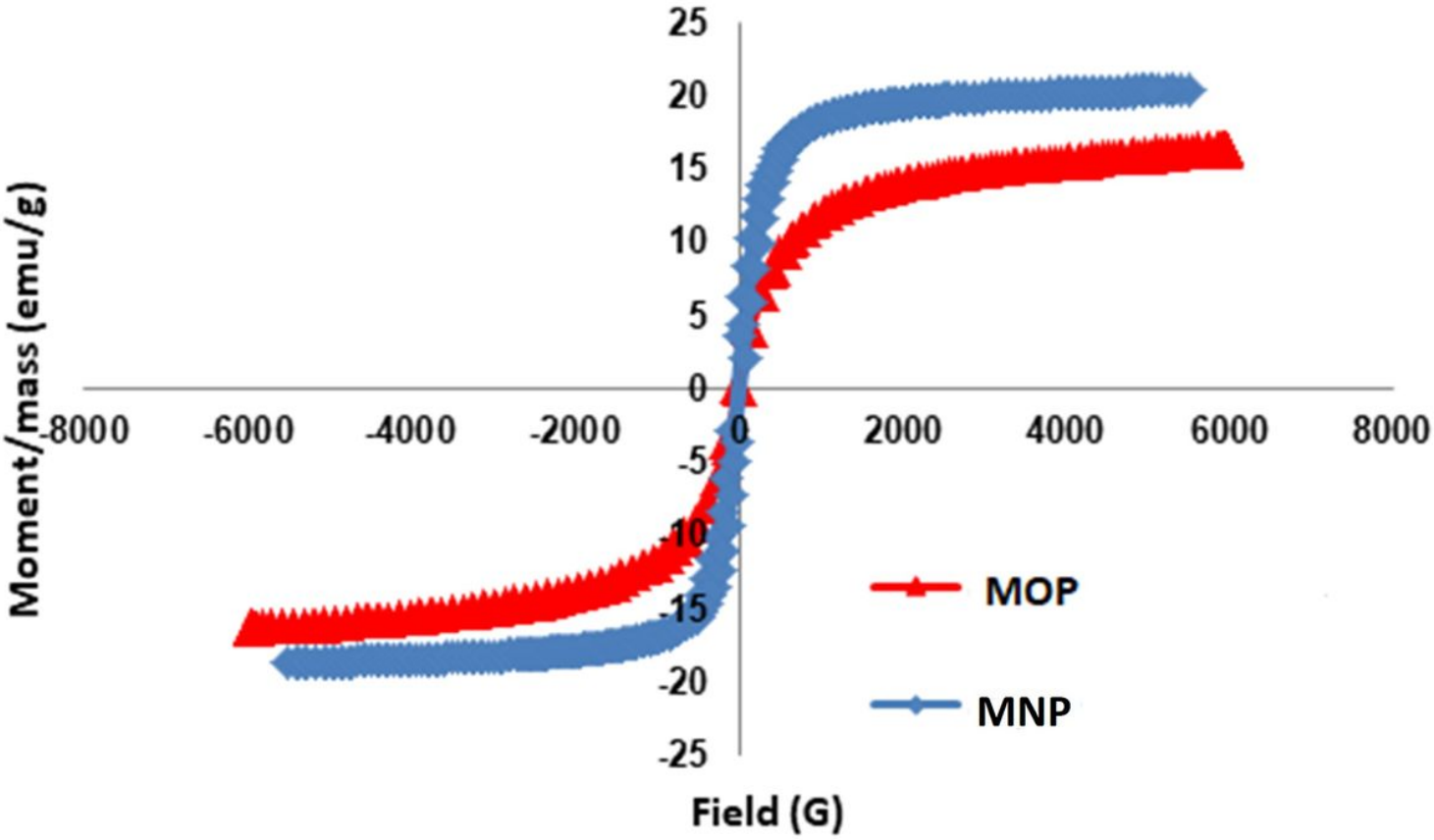

Figure 4

Hysteresis loops of the MNP and MOP

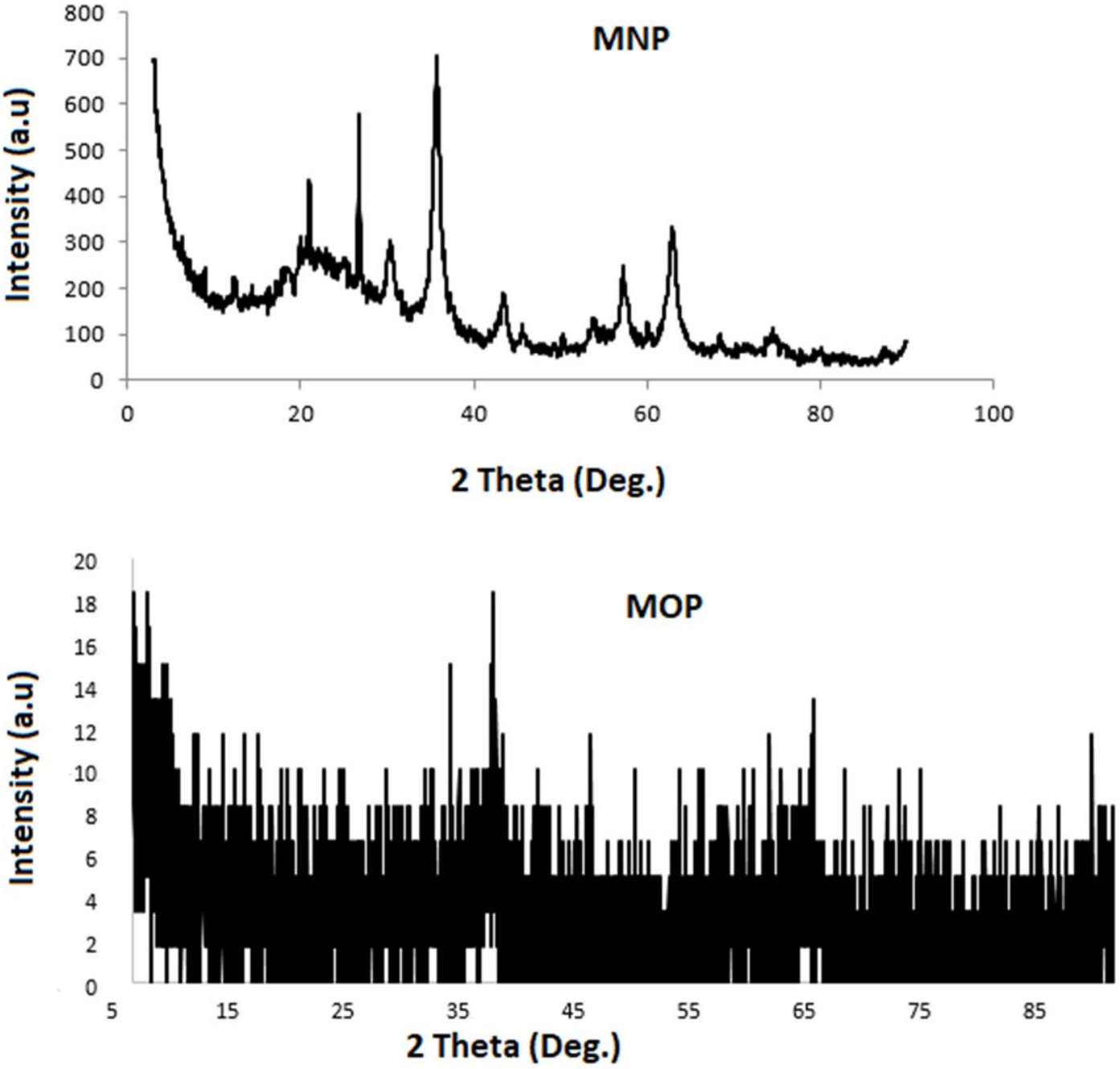

Figure 5

XRD pattern of the MNP and MOP

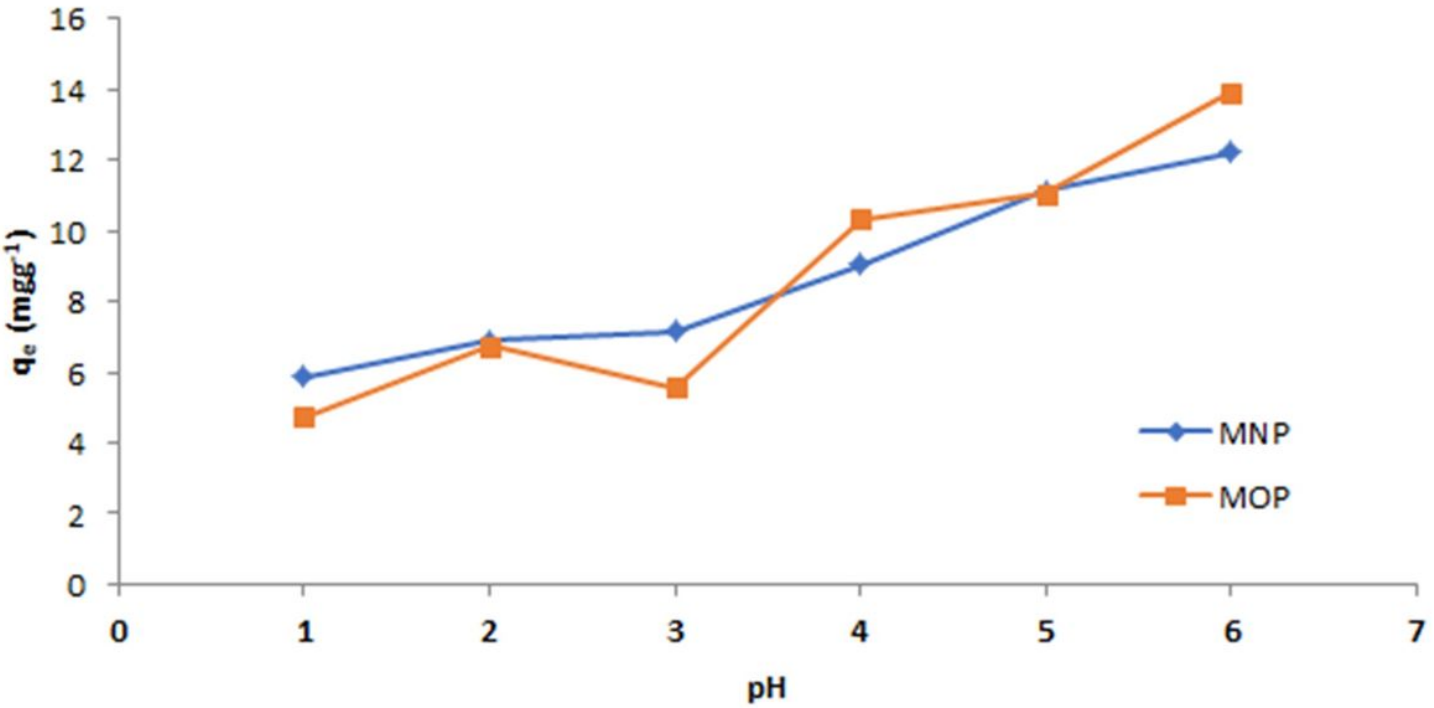

Figure 6

Influence of pH on sorption of Ce(III) ions by the MNP and MOP nanocomposite (m: 0.04 g, c: 100 mgL-1, v: 10 mL, t: 2 h)

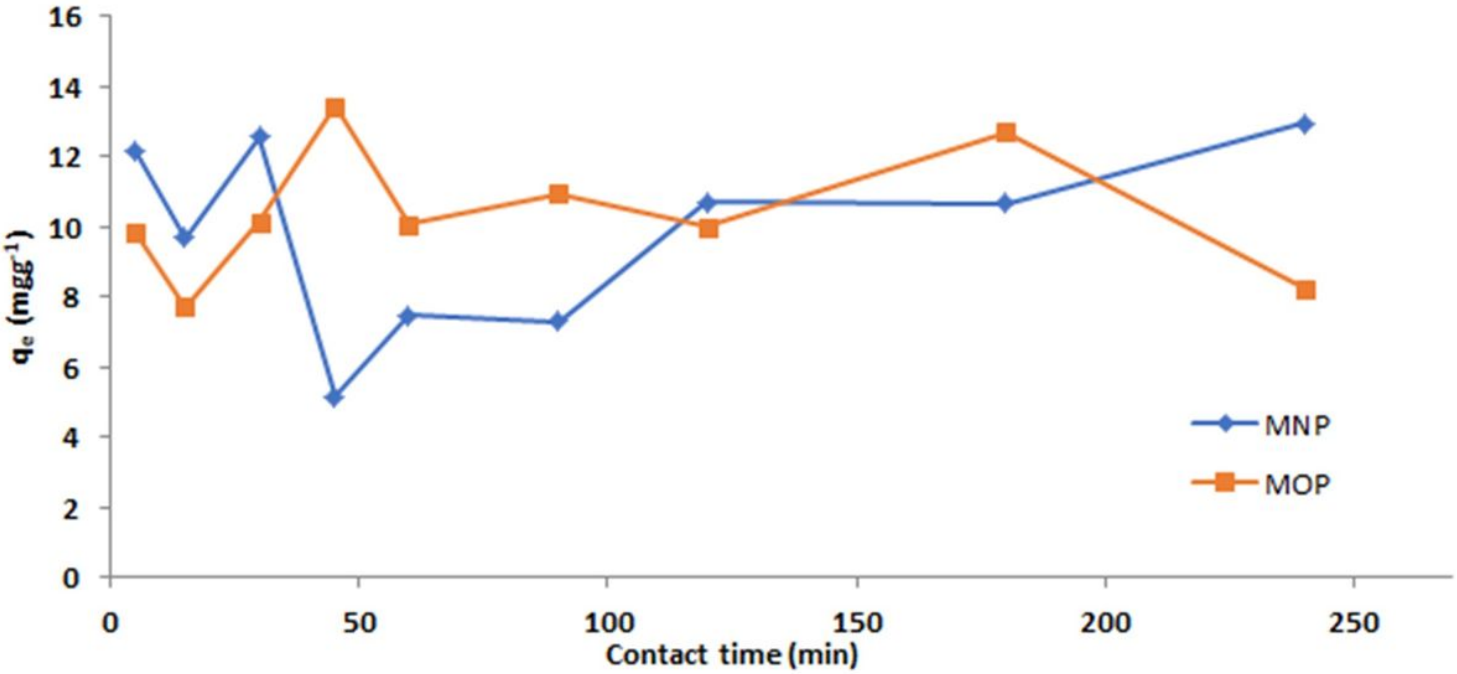

Figure 7

Influence of contact time on sorption of Ce(III) ions by the MNP and MOP nanocomposite (m: 0.04 g, c: 100 mgL-1, v: 10mL, pH:6.0)

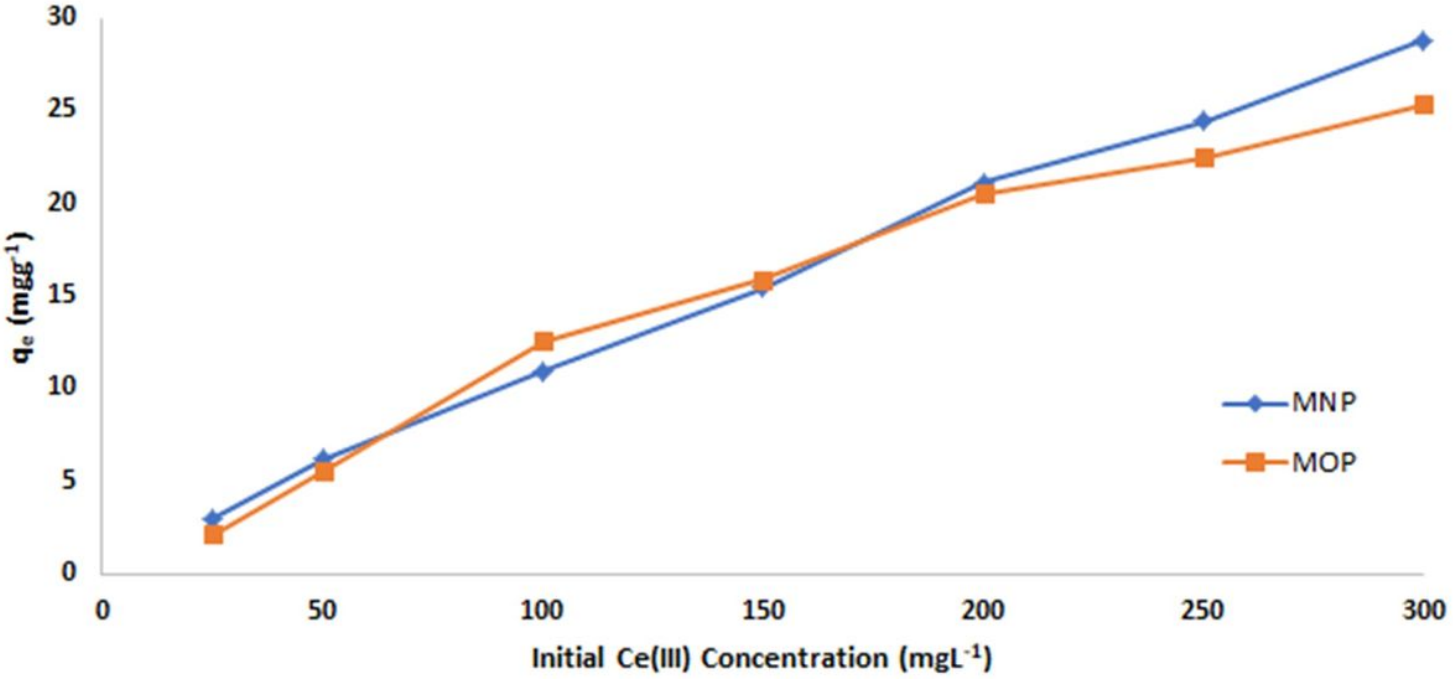

Figure 8

Influence of initial concentration of Ce(III)ions by the MNP and MOP nanocomposite

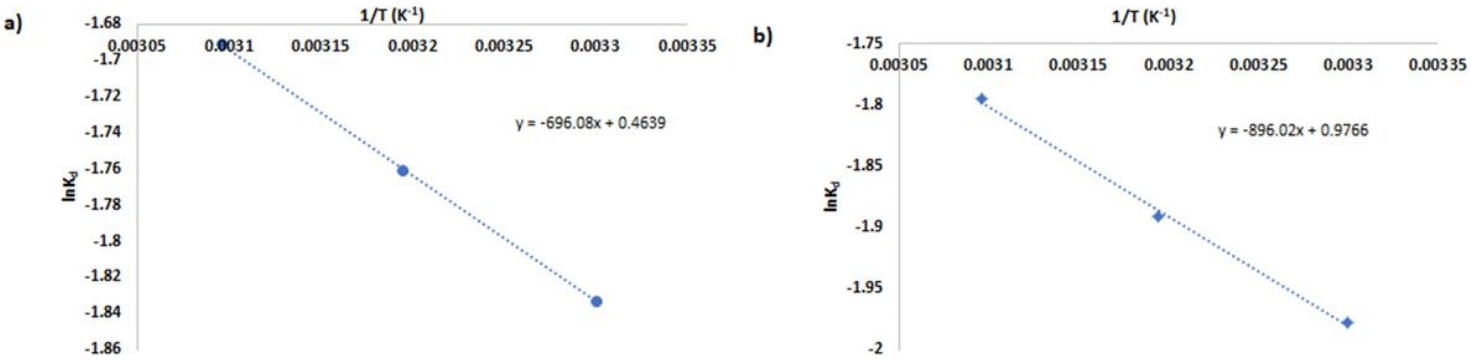

Figure 9

lnKd versus temperature graph of Ce(III) sorption by the MNP (a) and MOP (b) nanocomposite Table 1. Thermodynamics parameters of Ce(III) sorption

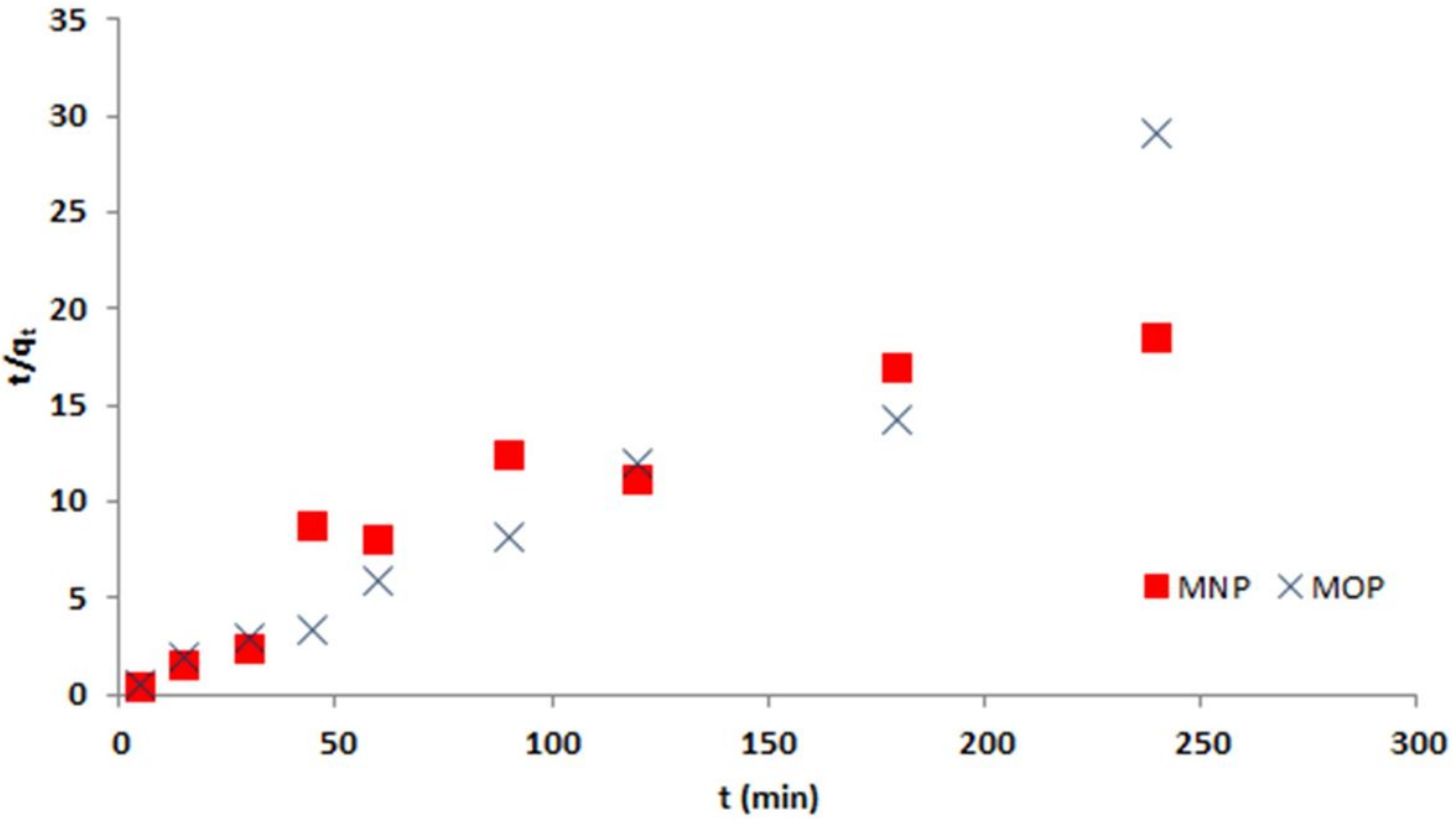

Figure 10

Plot of pseudo-second order kinetic model for sorption of Ce(III) onto MNP and MOP